Comparison of Time-Frequency Localization Methods and Spectral Evolution

Bruno S. Silva, Lourenildo W. B. Leite, Fernando T. B. Andrade, Adriany T. M. Reis, Wildney W. S. Vieira, UFPA, Brazil

Abstract

The main purpose in the present work is the comparison of some methods that can be applied for a time-frequency map distribution of seismic data, that is typically a multi-sensor technique. The generalized data attribute analysis is potentially a data-driven methodology to complement geological information for interpretation purpose. A seismic signal carries the information from the subsurface, and the goal is the oil and gas exploration in a porous and fractured medium. The propagating signal samples the geology by the transmission and reflection seismic fields, and the characteristics of the medium is present in the data under geometric and frequency properties. And the important principle underlying the $t-f$ decomposition is that an arbitrary signal is caused by a linear superposition of elementary wavelets, but goes further to an atomic decomposition, in the sense that of "well" localization in time and frequency.

Introduction

This work has for objective compare five time-frequency local spectral estimations to analyze the evolution as a possible measure of attributes characterization of a seismic trace, and for this we used a synthetic model where we can have control to configure the evolution and information localization. It has been published that time-frequency analysis as a temptative to characterize a subsurface geological model aiming oil and gas exploration, where the wave propagates in porous and fractured media.

Would it be possible to differentiate between geology formed of thin layers, thick layers, mixed layers, periodical stratigraphical environments using time-frequency attributes? Also, would it be possible to follow these environments throughout a basin? Besides that, would it be possible to detect and follow stratigraphical and structural formations and events, and paleovalleys? These are very important geological features, and the energy applied to geometrical attributes research development are aimed at these questions. Therefore, complementary forces have to be applied into the time-frequency studies.

Several models for attribute measures have been proposed with this aim in the core of the oil industry, and they be classified in general as spectral and geometrical methods, as described by Chopra and Marfurt (2012). It is fascinating that time-frequency attributes are well developed and applied in the medical and biological area (Boashash, 2003). Besides, this area of research has received lots of attention, what we can commemorate with Cohen (1995) as a reference bank of information.

The synthetic model obeyed the superposition principle, where the trace $s(t;\mathbf{x})$, at a certain distance from the source $\mathbf{x}$, is represented by:

$$s(t) = \sum_{n=1}^{n=M} w_n(t) * R_n(t;\mathbf{x}) + r_n(t;\mathbf{x}), \qquad (1)$$

where $w(t)$ is the effective propagating source pulse (a form of wavelet), $R(t;\mathbf{x})$ is the path reflectivity, and $r_n(t;\mathbf{x})$ the local additive noise. The physical model is described by a propagating vertical propagating plane wave front, over a set of homogeneous, isotropic, horizontal layers, over a half-space in the bottom, and a half-space on the top represented by the air. The governing equation corresponds to a similar case to the acoustic wave propagation.

The analysis applied to a single t-trace produces on $t-f$-map; therefore, for a complete $t-x$-seismic section (2D survey), the result will be a volume (attribute cube), where the objective is to follow the attribute pattern inside the profile. To be more specific, different sections can be cut through the attribute cube as desired for the interpretation. In case of a 3D survey, a multidimensional cube is produced.

Methodology

The transforms applied are resumed to the title Short-Time Fourier Transform (STFT), and the ones chosen for this study are briefly described in the sequel. Pretty much in all cases, the transform interpretation is that of a moving symmetric window over the trace, and the obtained information placed with respect to its center. It is important to emphasize that numerical methods participate in this kind of study in a very strong presence. The different transforms (distributions) used have been combined in a group called Cohen Class (Flandrin, 1999; Boashash, 2003).

Hilbert Transform

The first part corresponds of attribute analysis naturally goes to the of the infinite Cauchy-type principle value transform, that is defined for a single domain for tow complex functions φ and ψ as:

$$\psi(t) = \frac{1}{i\pi}\int_{-\infty}^{+\infty}\frac{\varphi(\tau)}{t-\tau}d\tau, \quad \varphi(t) = \frac{1}{i\pi}\int_{-\infty}^{+\infty}\frac{\psi(\tau)}{t-\tau}d\tau. \qquad (2)$$

The real (Rψ, Rφ) and imaginary (Iψ, Iφ) parts of φ and ψ are related to each other as (Zhdanov, 1988):

$$\mathrm{R}\psi(t) = \frac{1}{i\pi}\int_{-\infty}^{+\infty}\frac{\mathrm{I}\varphi(\tau)}{t-\tau}d\tau, \quad \mathrm{I}\varphi(t) = -\frac{1}{i\pi}\int_{-\infty}^{+\infty}\frac{\mathrm{R}\psi(\tau)}{t-\tau}d\tau. \quad (3)$$

$$\mathrm{R}\varphi(t) = \frac{1}{i\pi}\int_{-\infty}^{+\infty}\frac{\mathrm{I}\psi(\tau)}{t-\tau}d\tau, \quad \mathrm{I}\psi(t) = -\frac{1}{i\pi}\int_{-\infty}^{+\infty}\frac{\mathrm{R}\varphi(\tau)}{t-\tau}d\tau. \quad (4)$$

called Hilbert transform $H\{.\}$ pairs, and also directly related to causal signals (Mesko, 1984). For the trace $s(t)$, the objective is to have a form of measuring the instantaneous amplitude (IA), phase (IP) and frequency (IF), of the time series. The pair of $H\{s(t)\}$, in the time domain, is related to the Fourier transform $F\{.\}$ in the following form (Leite, 2015):

$$F\{H\{s(t)\}\}(f) = \sigma_{\mathrm{c}}(f)F\{s(t)\}(f) \quad (5)$$

where σ_{c} is the sign function in the complex domain expressed as,

$$\sigma_{\mathrm{c}}(f) = \begin{cases} +i, & \text{for } f<0, \quad i=\sqrt{-1} \\ 0, & \text{for } f=0 \\ -i, & \text{for } f>0 \end{cases} \quad (6)$$

The analytic signal is defined by the following composition:

$$z(t) = s(t) + is_{\mathrm{H}}(t) = a(t)e^{i\phi(t)}, \quad (7)$$

from where $a(t)$ is called the instantaneous amplitude (or the envelope), and $\phi(t)$ the instantaneous phase with this physical meaning, and given respectively by,

$$f(t) = \frac{1}{2\pi}\frac{d\phi(t)}{dt} \quad \text{and} \quad \phi(t) = \tan^{-1}\left[\frac{s_H(t)}{s(t)}\right]. \quad (8)$$

An important property of the analytical signal is of doubling the Nyquist frequency.

The Spectrogram

The STFT of a signal $s(t)$ by a moving window by $w(t)$, which is not related to the signal and arbitrary, is expressed as a time truncation in the Fourier symmetrical direct transform as (Goswami and Chan, 2011):

$$S_{\mathrm{TT}}(t,f) = \frac{1}{\sqrt{2\pi}}\int_{-\infty}^{+\infty} e^{-i2\pi f\tau}s(\tau)w(\tau-t)d\tau = W(f)\otimes S^*(f), \quad (9)$$

where t denote the time position of the moving window, $w(t)$, for the spectral localization of the dominant Fourier frequency component along the trace. The transform results in a correlation in the spectral domain between $W(f)$ and $S(f)$, that can represent limitations, and can usually be analyzed with numerical experiments for the case of any function (signal).

The spectrogram is defined by the power spectrum (modulus squared), and serves as reference for the other STFT and distributions; i. e.:

$$S_{\mathrm{S}}(t,f) = \left|\frac{1}{\sqrt{2\pi}}\int_{-\infty}^{+\infty} e^{-i2\pi f\tau}s(\tau)w(\tau-t)d\tau\right|^2, \quad (10)$$

that corresponds to a quadratic operation (external) where the phase information is not considered.

Trapezoidal-Triangular Transform

The Trapezoidal window can be expressed as:

$$w(t) = \begin{cases} 1, & |t| \le \frac{T_1-T_2}{2} \\ -\frac{|t|}{T_2} + \frac{T_1+T_2}{2T_2}, & \frac{T_1-T_2}{2} < |t| < \frac{T_1+T_2}{2} \\ 0, & |t| \ge \frac{T_1+T_2}{2} \end{cases} \quad (11)$$

for a normalized length $0-1$, and internal corners at T_1 and T_2. When $T_1 = T_2$, it must reduce to the case of a Triangular window given simply by:

$$w(t) = \begin{cases} 1-|\frac{t}{T}|, & |t|<T \\ 0, & |t|>T \end{cases} \quad (12)$$

Gabor Transform

This transform, GT, uses the Gaussian (bell-shape) window function, which is given by:

$$w(t) = \frac{1}{\sigma\sqrt{2}}e^{-\frac{t^2}{2\sigma^2}}, \quad (\sigma>0), \quad (13)$$

that has the important property of recovering the information at the center point (Leite, 2015), with applications in surface wave dispersion measurement.

Stockwell Transform

This transform, ST, has been communicated by Stockwell et al. (1996), that is formed by two compensating parts; one factor that amplifies with increasing f, and another that smooths out around the central point t, expressed in the symmetric form by:

$$S_{\mathrm{S}}(t,f) = \frac{1}{\sqrt{2\pi}}\int_{-\infty}^{+\infty} e^{-i2\pi f\tau}h(\tau)|f|e^{-\frac{1}{2}(\tau-t)^2f^2}d\tau. \quad (14)$$

Wigner Transform

This transform (also called Wigner-Ville transform or distribution,), WT, is an another rather special distribution reference, described by Cohen (1995), and applications given by Boashash (2003). It is written in the form:

$$S_{\mathrm{W}}(t,f) = \frac{1}{\sqrt{2\pi}}\int_{-\infty}^{+\infty} e^{-i2\pi f\tau}s\left(t+\frac{\tau}{2}\right)s^*\left(t-\frac{\tau}{2}\right)d\tau \quad (15)$$

which displays a form of mirror-image local correlation function exhibited by the complex conjugate $(*)$ of $s(t)$, to form a $t-\tau$ map:

$$C_{\mathrm{ss}}(t,\tau) = s\left(t+\frac{\tau}{2}\right)s^*\left(t-\frac{\tau}{2}\right), \quad (16)$$

As a result, the integrand corresponds to a quadratic operation (internal), which is similar to the spectrogram (external quadrature), but essentially different because it does not require a window in this definition. In the spectral domain, it can be written as,

$$S_{\mathrm{W}}(t,f) = F_\tau\{C_{ss}(t,\tau)\}. \quad (17)$$

The Pseudo-Wigner transform, PWT, Cohen (1995), follows as a version of the windowed WT, to emphasize

the information more around the local time, t, what is expressed by a truncation window $h(\tau)$:

$$S_{\mathrm{PW}}(t,f) = \frac{1}{\sqrt{2\pi}} \int_{-\infty}^{+\infty} e^{-i2\pi f\tau} h(\tau) s\left(t+\frac{\tau}{2}\right) s^*\left(t-\frac{\tau}{2}\right) d\tau. \quad (18)$$

In the experiments, the applied $h(\tau)$ was the Hamming window, as an option; but other functions can be equally tested as, for instance, the attractive Gabor window.

Choi-Williams Transform

This transform, CWT, is another special concept similar to the WV, described by Cohen (1995), with applications given by Flandrin (1999), and written in the following form:

$$S_{\mathrm{CW}}(t,f) = \sqrt{\frac{2}{\pi}} \int\int e^{-i2\pi f\tau} \frac{\sigma}{|\tau|} e^{-2\sigma^2 \frac{(\varsigma-t)^2}{\tau^2}} s\left(\varsigma+\frac{\tau}{2}\right) s^*\left(\varsigma-\frac{\tau}{2}\right) d\varsigma d\tau \quad (19)$$

where there is a window applied to the internal quadratic expression, for truncation and amplification with τ,

$$C_{\mathrm{CW}}(t,\tau) = \frac{1}{|\tau|} e^{-2\sigma^2 \frac{(\varsigma-t)^2}{\tau^2}} s\left(\varsigma+\frac{\tau}{2}\right) s^*\left(\varsigma-\frac{\tau}{2}\right). \quad (20)$$

As a result, which is similar to the spectrogram, but essentially different where the integrand corresponds to a quadratic operation (internal). In the spectral domain can be simplified to

$$S_{\mathrm{CW}}(t,f) = F_\tau\{C_{\mathrm{CW}}(t,\tau)\}. \quad (21)$$

A non-desired property of the WV and CW distribution is due to crossing terms.

Cross Terms

An important part of the analysis in the general Cohen Class is the presence of cross terms that make the transform rather complex, and as a resume of this is to look at the the WT of (1), where the observed signal is constructed by the sum of several atom contributions (Cohen, 1995), simplified to a simpler case without the presence of the noise term, and considering the total signal as the contribution of atom components, as expressed by:

$$s_{\mathrm{T}}(t) = \sum_{n=1}^{n=M} w_n(t) * R_n(t;\mathbf{x}) = \sum_{n=1}^{n=M} a_n s_n(t;\mathbf{x}). \quad (22)$$

Inserting in the WT, the result is given by the expression:

$$S_{\mathrm{WT}}(t,f) = \sum_{n=1}^{n=M} |a_n|^2 S_{\mathrm{W}n}(t,f) + \mathrm{I}_n^M(t,f), \quad (23)$$

where the interference term, I_n^M, is given by

$$\mathrm{I}_n^M(t,f) = 2 \sum_{n=1}^{n=M-1} \sum_{k=n+1}^{n=M} \mathrm{R}\{a_n a_k^* S_{\mathrm{W}n}(t,f)\}, \quad (24)$$

that shows that the WT contains $M(M-1)/2$ additional terms for a signal composed of M individual contributions, that result from the bilinear structure. In expression (23), the real term $\mathrm{R}\{a_n a_k^* S_{\mathrm{W}n}(t,f)\}$ corresponds to a modulation due to the presence of the cosine function.

To visualize better, the specific case of only two components,

$$s(t) = s_1(t) + s_2(t), \quad (25)$$

since by symmetry, $S_{12} = S_{21}^*$, and $S_{12} + S_{21} = 2\mathrm{R}\{S_{12}\}$, the result is simplified to:

$$S(t,f) = S_{11}(t,f) + S_{22}(t,f) + 2\mathrm{R}\{S_{12}\}. \quad (26)$$

And for a classical illustrative example, the signal composed by two complex exponentials:

$$s(t) = A_1 e^{i2\pi f_1 t} + A_2 e^{i2\pi f_2 t}, \quad (27)$$

that has for result,

$$\begin{aligned} S(t,f) &= A_1^2\delta(f-f_1) + A_2^2\delta(f-f_2) \\ &\quad + 2A_1A_2\delta(f-\frac{f_1+f_2}{2})\cos[(f_1+f_2)t] \end{aligned} \quad (28)$$

that shows concentrations at $f=f_1$ and $f=f_2$ in the main term, and also some information at the average frequency $f=\frac{f_1+f_2}{2}$ from the interference term. That is an important point in data processing involving $t-f$ analysis.

The variants to the WV transform also present the cross terms, and the ones with applied windows (smoothing and amplification) are attempts to attenuate the cross term effects, but also attenuates the main information.

Results

The strategy applied for the comparison of the time-frequency adapted distributions followed the original work of Steeghs and Drijkoningen (1995), where several models were considered corresponding to geological situations. In all cases, first the models were considered without noise, and then different levels of noise were imposed. The cases modeled sedimentary basins, where the velocity distribution varied slowly with depth based on empirical models, with the layers imposing randomness. Figure 1 shows the adopted data model for exemplification, that was obtained from the open data set from Keys and Foster (1998). The Matlab (www.mathworks.com), and associated (see Octave, www.gnu.org), and other individual contributions are present in the web covering some of these computer developments (Chopra and Marfurt, 2012).

Figure 2 shows the Ricker wavelet with dominant frequency of 25 Hz (index number $n=64$), used in the modeling shown examples.

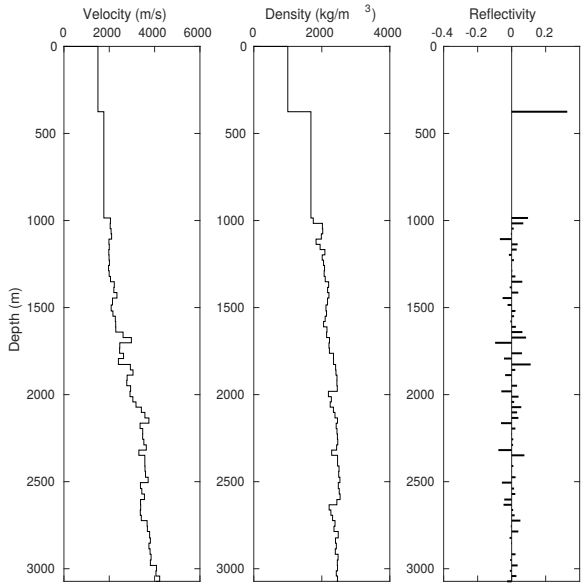

Figure 1: Geological Model given in three parts.

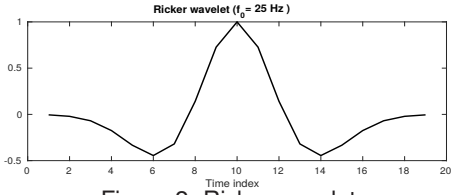

Figure 2: Ricker wavelet.

Figure 3 shows the desired products from the Hilbert transform and the analytic trace without noise, displaying the trace with the superposed envelope, followed by the instantaneous frequency (IF) and phase (IP). We intentionally left the numerical noise present in the IF, due to the computation of the derivatives over the IP curve, as one can see, and calculated by formulas 8.

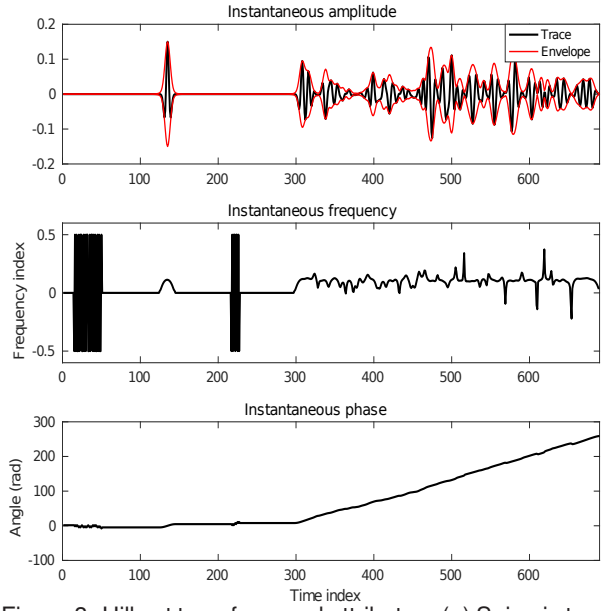

Figure 3: Hilbert transform and attributes. (a) Seismic trace and instantaneous amplitude. (b) Instantaneous frequency. (c) Instantaneous phase.

Figure 4 show the $t-f$ maps for the Triangular, Trapezoidal, Gabor and Stockwell window, with the respective Fourier transforms, for the case of noiseless trace, where we can observe the similar evolution in the spectrum. The width of the applied windows corresponded to the length of the used Ricker pulse.

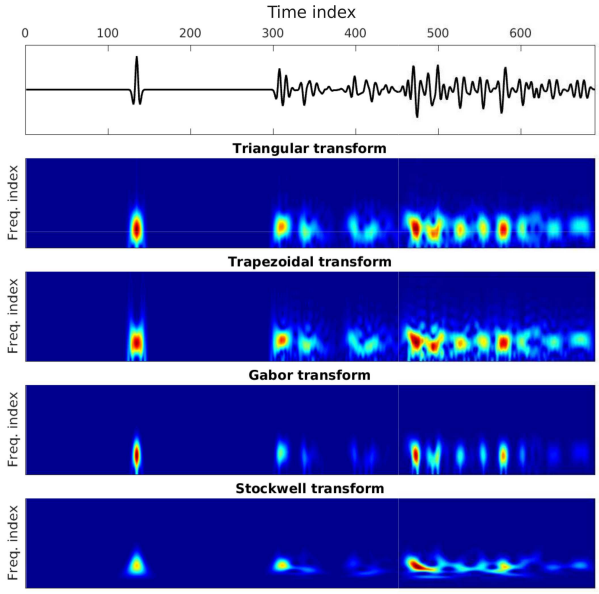

Figure 4: (a) Seismic trace. Windows and Fourier transform: (b) Triangular. (c) Trapezoidal. (d) Gabor. (e) Stockwell.

Figure 5 shows the maps for the Wigner-Ville and Pseudo Wigner-Ville correlation distributions ($t-\tau$), and the respective Fourier transforms ($t-f$) for the noiseless trace, where the effect of the weighting Hamming window applied is very clear for attenuating the artifacts (crossing terms).

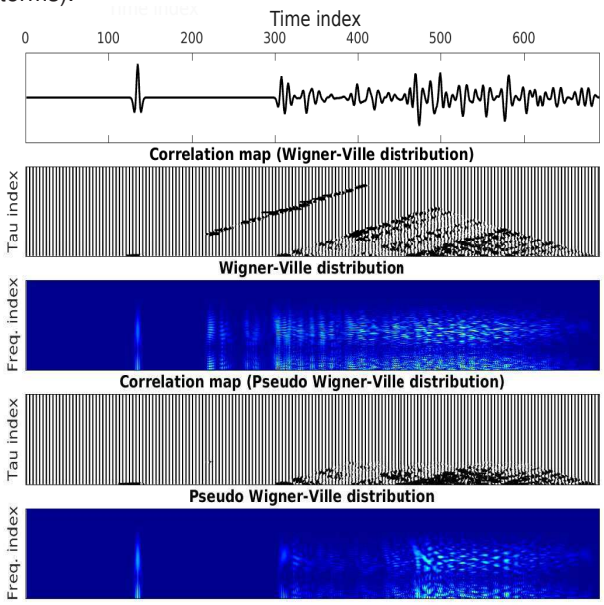

Figure 5: (a) Seismic trace without noise. Distributions: (b) Correlation map of the Wigner-Ville. (c) Wigner-Ville. (d) Correlation map of the Pseudo Wigner-Ville. (e) Pseudo Wigner-Ville.

Figure 6 shows the maps for the Choi-Williams correlation distribution ($t-\tau$) and the Fourier transform ($t-f$) for the

noiseless trace. It is clear how some distributions can be compared to the Pseudo Wigner-Ville and plain Wigner-Ville transforms, but stronger in localizing frequencies.

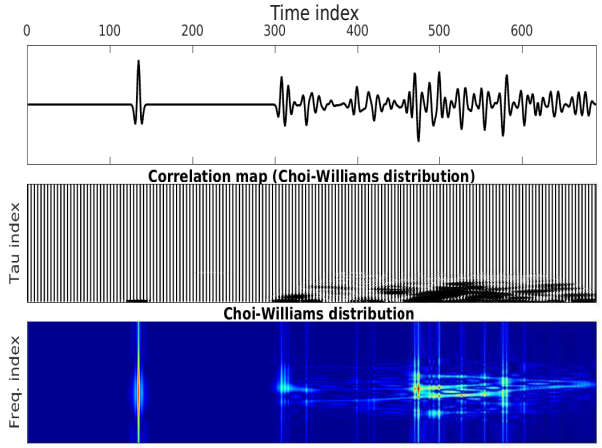

Figure 6: (a) Seismic trace without noise. Distributions: (b) Correlation map of the Choi-Williams. (c) Choi-Williams.

Figure 7 shows the products of the Hilbert transform and analytic trace with noise, displaying the trace with the superposed envelope, followed by the IF and IP curves. Again, we show an example where the numerical noise is strongly present in the IF, due to the computation of the derivatives over the IP curve, and calculated by formulas 8. The IF curve shows a very complex (noise) pattern; in the other hand, the IP curve still looks well behaved, and potentially useful.

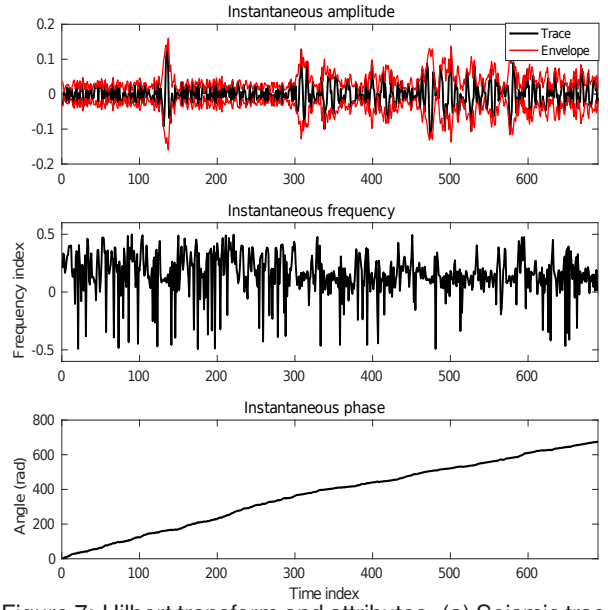

Figure 7: Hilbert transform and attributes. (a) Seismic trace with noise and instantaneous amplitude. (b) Instantaneous frequency. (c) Instantaneous phase.

Figure 8 show the $t-f$ maps for the Triangular, Trapezoidal, Gabor and Stockwell window and respective Fourier transforms, for the case of noisy trace, where we can see that it is more complex than for figure 4, and not much difference in the spectral evolution, with small details.The width of the applied windows correspond to the length of the propagating pulse.

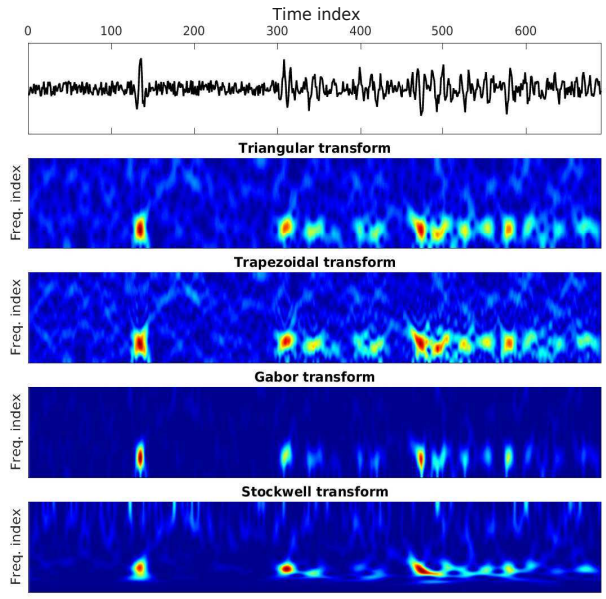

Figure 8: (a) Seismic trace with noise. Windows and Fourier transform: (b) Triangular. (c) Trapezoidal. (d) Gabor. (e) Stockwell.

Figure 9 shows the maps for the Wigner-Ville and Pseudo Wigner-Ville correlation distributions $(t-\tau)$ and their respective Fourier transforms $(t-f)$ for the noisy trace, where the effect of the weighting Hamming function is very clear is attenuating the artifacts (crossing terms).

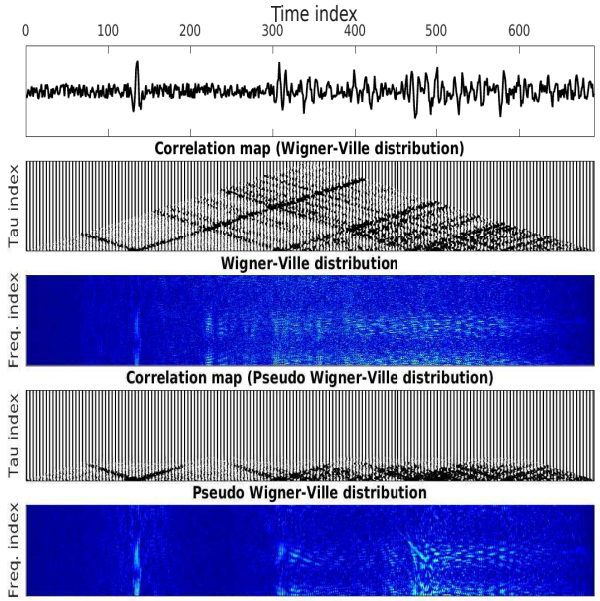

Figure 9: (a) Seismic trace with noise. Distributions: (b) Correlation map of the Wigner-Ville. (c) Wigner-Ville. (d) Correlation map of the Pseudo Wigner-Ville. (e) Pseudo Wigner-Ville.

Figure 10 shows the maps for the Choi-Williams correlation distribution $(t-\tau)$ and the Fourier transform $(t-f)$ for the noisy trace.It is also clear how the distribution can be compared to the Pseudo Wigner-Ville and plain Wigner-Ville transforms in localizing frequencies, but now the details are very sharp due to the applied exponential window.

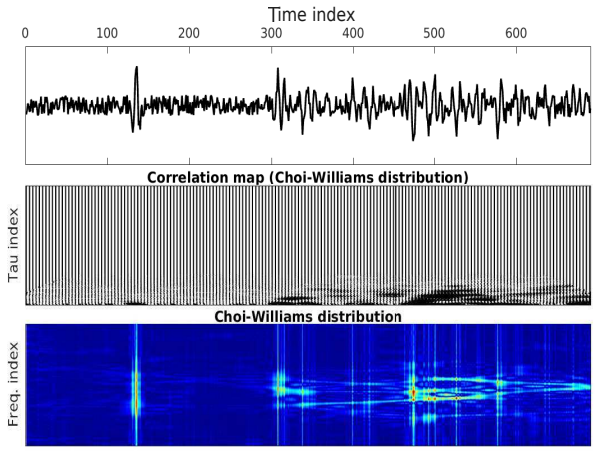

Figure 10: (a) Seismic trace with noise. Distributions: (b) Correlation map of the Choi-Williams. (c) Choi-Williams.

Conclusions

The Hilbert transform and analytical signal can impose a very complex and noisy IF curve, but the IA and IP are rather smooth and useful.

In order to establish the capability of the short-time and quadrature distributions in detecting the spectral evolution, it is clear that it is necessary to first classify the signal trace with respect to message and noise components. And also to have the goals very clear, due to the fact of many possibilities present in the Cohen class.

Numerical experiments and theorectical models are important for obtaining results that can have practical use in characterizing structures in the subsurface.

It is necessary a proper parametrization of the maps for being able to see details of the different $t-f$ methods, but has not been the case here to choose the best representation. But we can emphasize that the presence of a truncating window, $t-\tau$, on the Wigner-Ville quadrature principle can be very attractive for localizing frequencies in a data processed cube.

The attractive Wigner-Ville transform call for more attention, and naturally further research work must be oriented towards analyzing and masking (filtering) the interference terms (considered as artifacts).

References

Boashash, B., 2003, Time frequency signal analysis and processing: Elsevier, Amsterdam, Holanda.

Chopra, S., and Marfurt, K. J., 2012, Seismic attributes fo prospect identification and reservoir characterization: SEG Geophysical Developments Series No. 11, Tulsa, USA.

Cohen, L., 1995, Time-frequency analysis: Prentice-Hall, New Jersey, USA.

Flandrin, P., 1999, Time-frequency time-scale analysis: Academic Press, New York.

Goswami, J. C., and Chan, A. K., 2011, Wavelets theory, algorithms, and applications: Wiley, New Jersey, USA.

Keys, R., and Foster, D., 1998, A data set for evaluating and comparing seismic inversion methods *in* Keys, R., and Foster, D., Eds., Comparison of seismic inversion methods on a single real data set:: Society of Exploration Geophysicists, 1–12.

Leite, L. W. B., 2015, Conceitos da análise espectral de sinais em geofísica: Instituto de Geociências, UFPA, Belém, Pará.

Mesko, A., 1984, Digital filtering: Applications in geophysical exploration for oil: Pitman Advanced Publishing Program, Londres.

Steeghs, P., and Drijkoningen, G. G., 1995, Time-frequency analysis of seismic sequences: SEG Techcnical Program Expanded Abstracts. http://dx.doi.org/10.1190/1.1887266, **1**, 1528–1531.

Stockwell, R. G., Mansinha, L., and Lowe, R. P., 1996, Localization of complex spectrum: the S transform: IEEE Transactions on Signal Processing, **44**, 998–1001.

Zhdanov, M. S., 1988, Integral transforms in geophysics: Springer-Verlag, Berlin, Germany.

Acknowledgments

The authors would like to thank the sponsorship of Project INCT-GP and to the Project ANP-PRH-06, that are present in part of the sponsorship of this research work. We extend our thanks also to CAPES and CNPQ for the student scholarships.